AIAA 2000-4419
Airfoils with Dynamic Transonic Flow Control

M. Trenker, W. Geissler and H. Sobieczky
DLR German Aerospace Center

18th AIAA Applied Aerodynamics Conference

Aug. 14 - 17, 2000
Denver, CO

AIRFOILS WITH DYNAMIC TRANSONIC FLOW CONTROL

M. Trenker*, W. Geissler, H. Sobieczky*****
DLR German Aerospace Center
Institute of Fluid Mechanics
Dept. High Speed Aerodynamics
D-37073 Göttingen, Bunsenstr. 10
Germany

Abstract

Design modifications to airfoils in unsteady transonic flow are carried out by means of realistic geometry modeling and systematic transonic design removal of recompression shocks. Results of systematic design lead to simplified shape modification functions shortcutting the use of 2D steady and unsteady numerical methods and help extending design knowledge base to improving airfoils for helicopter rotors and dynamic stall control.

Introduction

In recent past years practical concepts to adapt aerodynamic components of flight vehicles in transonic speed for varying operating conditions have gained renewed attention after years when theoretical methods [1], [2] already suggested systematic shape variations to airfoils and lifting wings.

New materials, refined control mechanisms and more stringent requirements to reduce fuel consumption have led to several concepts to modify efficient flow boundaries during flight by elastic, pneumatic, piezoelectric and other devices so that there is a realistic chance now that one of these technologies will in some way lead to improvements of a commercial product.

In this situation theoretical and numerical analysts are challenged to refine their tools to better model geometrical boundary conditions including mechanical constraints [3], and use advanced numerical analysis to fully model viscous effects in compressible flow. The latter is to be developed especially for simulation of unsteady flow phenomena in transonic flow, since it seems that the periodic performance of helicopter rotor blades, including the occurrence of dynamic stall, may be influenced most favorably by adaptive devices.

In consequence of these developments, we have updated software for geometric preprocessing of 2D and 3D configurations, as well as for numerical analysis, to generate and simulate airfoils in unsteady shape and flow conditions. First results of improved aerodynamic performance have been obtained by combining a large camber modification of a standard airfoil with local contour flattening based on the transonic design knowledge base [4].

In this contribution we arrive at exploring different models for camber variation. Not only the portion of the modified airfoil parts but also analytical models used for airfoil deformation will be tested with a view to effectiveness in flow control and mechanical realization.

Although the lowest free stream Mach number is lower than $M = 0,3$ transonic flow considerations are necessary since even at this low Mach number there are supersonic regions on the airfoil which have a strong effect on flow characteristics, [7].

Also, we try to investigate the role of systematic shock-free redesign, comparing a steady, inverse method of characteristics with simplified geometry modifications guided by the Fictitious Gas (FG) design method.

The geometry models will be analyzed under an oscillatory motion together with phase-shifted variation in Mach number. This will be done regarding to an industrial application in the field of helicopter aerodynamics.

The flowfield response to our geometric investigations will be numerically solved by our 2D-time accurate implizit Navier-Stokes Code which features the most common turbulence- and transition-models.

Here the importance of adequate turbulence models as well as appropriate models for transition will be pointed out if the aim is predicting heavily separated flows at low Mach numbers as well as flows in the transonic speed regime.

In [8] detailed comparisons of computed fully turbulent and transitional flow solutions with experimental data are presented.

---

* Research associate

** Sr. research scientist, Member AIAA

*** Professor, Assoc. Fellow AIAA

Defining a new airfoil for a selected design point

The correlation of the angle of attack (AoA) and the phase-shifted variation in Mach number (M) will be defined in dependence of the dimensionless time (T) as depicted in Fig.1.

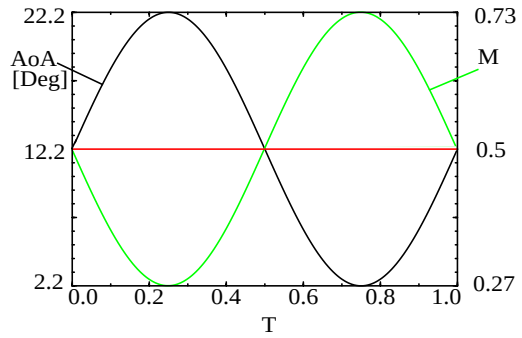

Fig.1 Relation between angle of attack (AoA) and Mach number (M)

In order of creating a new airfoil we define our design-point at $T = 0{,}75$. Here the AoA reaches its minimum value of $AoA = 2,2Deg$ corresponding to the highest Mach number which is in our case $M = 0{,}73$.

We use our geometric preprocessing tools to create an initial airfoil of the 'PARSEC' family [3] as a suitable starting configuration for adaptive helicopter rotor blade design. Systematic shock-free redesign to remove the shock at design conditions, Fig.2(a), based on the FG-design method combined with an inverse method of characteristics (IMOC) applied to the supersonic region of the flowfield (Fig.3) results in an intermediate design, Fig.2(b), optimized for design values. A relaxation of surface modification parameters leads to the final airfoil, further used in this paper as 'baseline rigid airfoil', Fig.2(c) with $c_l = 0,5$, $c_d = 0,011$, $c_m = -0,04$. This final variation was found useful especially for unsteady flows providing an airfoil suitable for a whole range of flow parameters varying in the vicinity of design conditions.

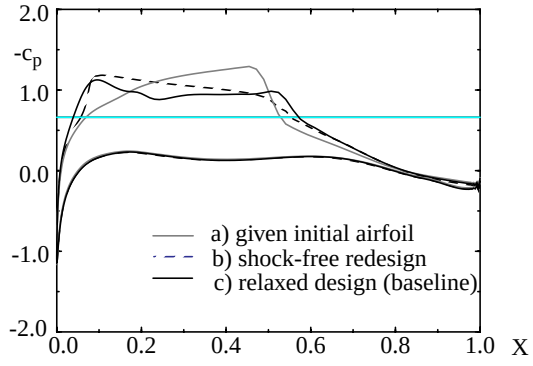

Fig.2 Pressure distributions for given and redesigned airfoils using steady fully turbulent Navier-Stokes calculations

Using the FG-method the real flowfield around the airfoil is computed except at regions where the local flow velocity exceeds the critical speed. In potential theory for ideal gas this region would be modelled by some hyperbolic partial differential equation (PDE). However, the FG-method solves an elliptic PDE everywhere in the flowfield. This leads to solutions for the usual, ideal gas in regions with subsonic speeds and a solution in the formally supersonic region, but for a fictitous gas.

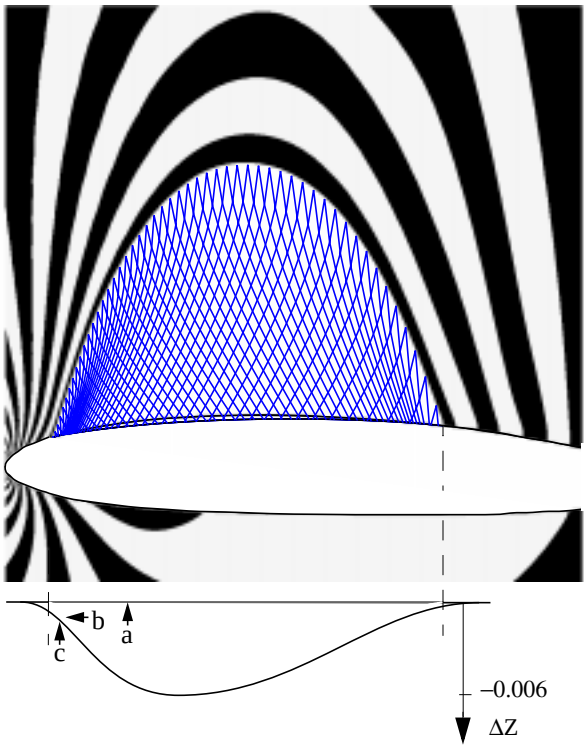

Fig.3 Isobars at design conditions; steady 2D flow characteristics as derived from IMOC starting at the critical pressure line and defining the new contur. Subtracted surface bumps refer to Fig. 2

Since recompression shocks are not possible in elliptic flows we achieve a shock-free flow model, Fig.3. For determining the real flow characteristics in the region surrounded by the sonic line we use our IMOC which needs flow data at the sonic line as initial conditions for marching toward the airfoil, to find its new contour compatible to the smooth sonic line. After taking into account some corrections for the boundary layer thickness we arrive at the new shock-free airfoil, Fig.4.

For a more deepened insight in the FG-method and the IMOC refer to [5], [6].

We have extended the 2D time-accurate Navier-Stokes code to allow for FG models, but for theoretical completeness we still have to show the potential of an unsteady method of characteristics.

For practical purposes, however, we use already unsteady, calibrated bumps derived from steady design, to adapt a shape dynamically to unsteady operating conditions.

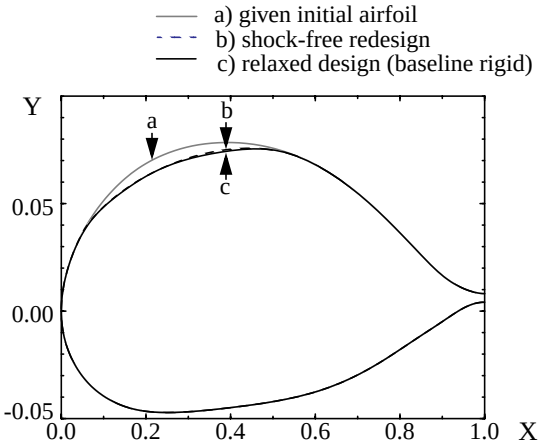

Fig.4 Design modifications on the airfoil contour, lines corresponding to Fig.2 (Scaled)

Models for airfoil deformation

An exact definition of flow boundary conditions by mathematically explicit functions has proven most beneficial for the quality of any numerical simulation. This is especially true if the goal of the analysis is finding shape modifications for improved aerodynamics. We use, therefore, analytical tools for input preprocessing prior to CFD. In the present case we like to investigate 2 possibilities for an airfoil deformation, which varies in time.

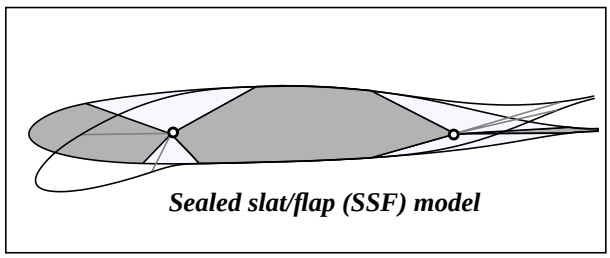

Fig.5 Airfoil modification by modeling a sealed slat and flap.

Rotation of rigid airfoil front or rear parts around given hinge points and their elastic connection, Fig.5, which is modeled by a quintic spline, is one way to define some unsteady boundary condition. Such a model of sealed slats and/or flaps with a smooth curvature connections may be realized mechanically.

Being in a position to actually choose all the necessary parameters rather freely in order to optimize unsteady flow quality gives us the chance to not only fulfill conditions which may be set by (present) industrial relevance, but also to take these as a starting point for finding new specifications for new parameters and defining their range regardless of present status of mechanical realization.

This was the motivation for finding an alternate way to define some effective parameters for creating airfoil deformation specification. As well known from classical aerodynamic theory used for defining airfoils in incompressible, inviscid, irrotational flow, airfoils can be defined as being composed by a camber line and a superimposed thickness distribution. According to that we can define some airfoil deformation by keeping control over the camberline shaping leaving the thickness distribution unchanged during deformation, Fig.6.

What is needed in this case is information about the camberline of the initial airfoil to be deformed.

Compared to resulting non-smooth local camberline shape distribution in Fig.5 in the hinge point area if slat and flap are rotated, the new model employs a smooth function for the camber line.

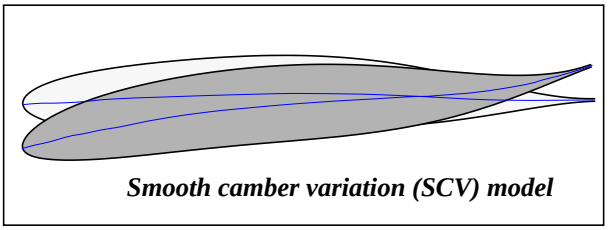

Fig.6 Airfoil modification by controlling the airfoil camber line

Modeling the camber line with some cubic function gives us the ability to closely fit the new (SCV-) airfoil to the previous (SSF-) airfoil variation.

As mentioned in the introduction we think of our geometry definitions as being part of the geometry preprocessing which itself is part of the design toolbox finally becoming part of some mechanical realization software.

However, in order of judging a geometry model and the choice of adequate parameters it is not sufficient to restrict the view on geometry. Rather a multidisciplinary view is needed, at least for structural concerns, in order to decide which model actually fits a certain application.

Flow solver conditions

For the flow solver the use of a structured cartesian grid of the dimensions (385×81) was found suitable. The smallest grid element height is found in the first layer with a $\Delta = 2 \times 10^{-5}$ referred to chord (c).

The choosen reduced frequency was set to $\omega^* = 0,1$ which results for a Reynolds number of $Re = 8 \times 10^6$ and the design Mach number of $M = 0,73$ in an oscillatory frequency of about $f = 7Hz$.

Case studies

First, we like to investigate our baseline rigid airfoil under unsteady flow conditions as depicted in Fig.1. To illustrate the flow quality we use 3D graphics as shown in Fig.7 with the axes in (X,Time, -c_p) directions.

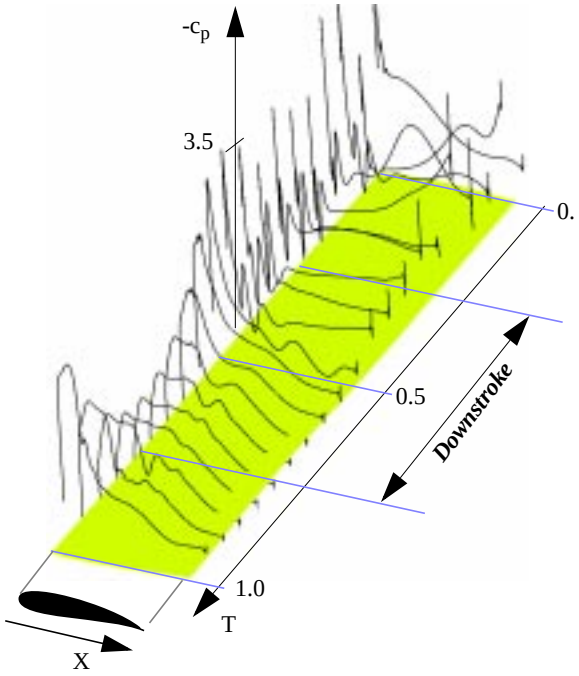

Fig.7 Pressure coefficient for the baseline rigid airfoil upper surface under unsteady conditions. Fully turbulent, Spalart/Allmaras turbulence model

The illustration starts at the mean angle of attack of $AoA = 12,2Deg$ and a Mach number of $M = 0,5$. We have some high suction peaks because of strong acceleration starting from the stagnation point. Strong separation on the airfoil upper surface is taking place as the airfoil moves towards the highest AoA and accordingly the lowest Mach number at $T = 0,25$. The shedding of the dynamic stall vortex can be seen as a wave being transported toward the trailing edge and subsequently into the wake of the airfoil. As the airfoil moves towards its lowest AoA at $T = 0,75$ to reach the steady flow design point we realize not only nearly shock-free flow but a whole region around the design point with very weak shock strength.

This flow characteristics confirms us in using a steady design method also for unsteady flows as long as the reduced frequency ω^* is not too high.

However for suppressing effects like the strong separation on the upper airfoil side we like to test our geometry models for effectiveness. Some work in this field was done recently [10] where we limited the size of the sealed slat to 10% chord at the nose, and no sealed flap, for industrial relevance.

To show the potential of deforming airfoils we now like to allow for larger deformations.

We defined a deformation using the SSF model according to Fig.5 with large elastic connections and reduced rigid portions of the contour, Fig.8

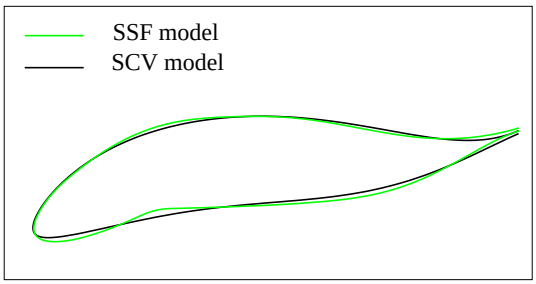

Fig.8 Airfoils at maximum deformation (scaled)

For comparing purposes we also modeled an airfoil according to the SCV geometry (Fig.6) by aiming to achieve nearly the same (maximum) deviation at airfoil leading edge and trailing edge as achieved with the SSF model according to Fig.5.

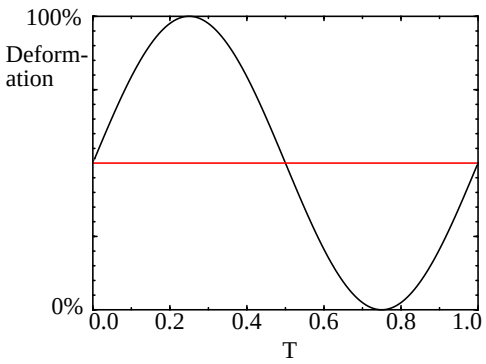

Fig.9 Airfoil deformation vs. dimensionless time, to be seen in conjunction with Fig.1

The airfoil deformation is in phase with the AoA variation as is illustrated in Fig.9 which is to be related to Fig.1.

Deforming the initial airfoil according to the SSF model shows improvements of the flow quality over most of the airfoil upper surface:

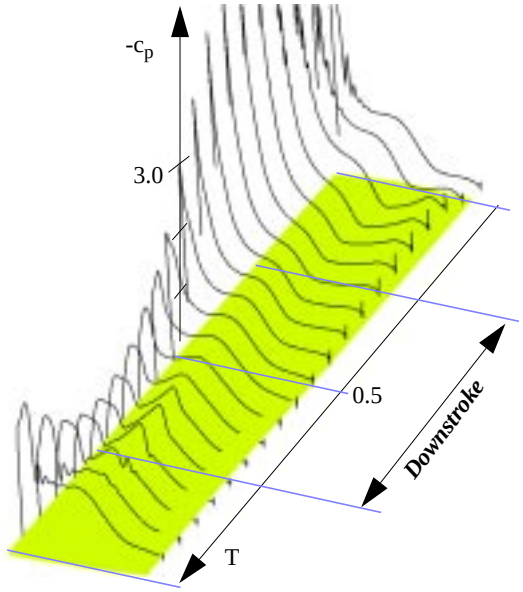

Fig.10 Pressure coefficient for the deforming SSF airfoil upper surface. Fully turbulent, Spalart/ Allmaras turbulence model

As seen in Fig.10 this model is able to achieve dramatically improved pressure distributions in the time domain T < 0.5 compared to Fig.7, at the expense of a breakdown of the shock-free domain at T ~ 0.75: the elastic contour connection modifies the designed shape enough to result in a double shock c_p distribution. A fully 2D-unsteady flow shock-free redesign method with a refined elastic connection fit between drooped nose and rigid airfoil mainframe could cure this setback, software development for these improvements still has to be done.

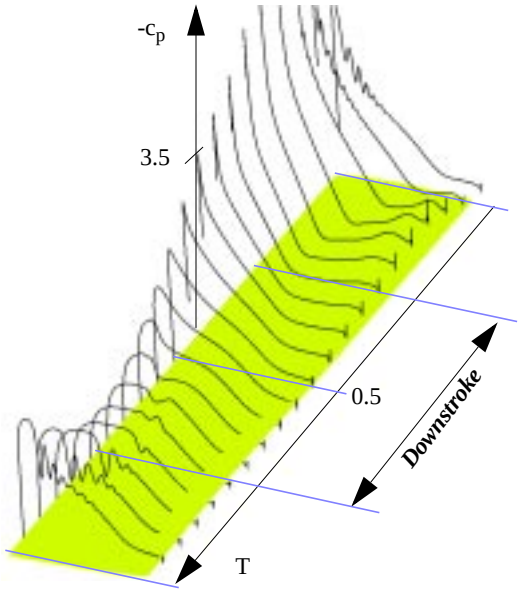

Fig.11 Pressure coefficient for the deforming SCV airfoil upper surface. Fully turbulent, Spalart/ Allmaras turbulence model

Systematic shock-free redesign establishes a curvature balance on the upper airfoil surface which is likely to be disturbed by a mechanical device for a sealed slat. The following result, Fig.11, computed for the smoother SCV airfoil, happens to suit a shock-free flow much better, as can be seen in the c_p distribution in the T ~ 0.75 area in Fig.11. Modified curvature due to the distributed camber deformation leads to sonic flow conditions closer to the airfoil nose and subsequent smooth curvature reduction accomodates a 'rooftop' pressure distribution with a nearly absent recompression shock. For T ~ 1 we see that the shock breaks up into a series of waves.

To judge the overall performance of airfoil deformation models we use c_l, c_d, c_m versus AoA plots, as depicted in Fig.12 to Fig.14.

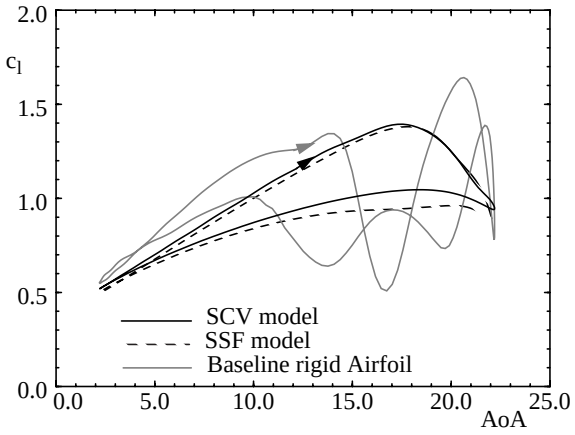

Fig.12 Lift coefficient vs. AoA for rigid airfoil, SSF and SCV airfoils

Both geometry models deliver clean curves for c_l-, c_d- and c_m, with a maximum in c_l which is about three times higher than the static value. Due to vortex shedding a loss in c_l occurs near the maximum AoA resulting in a hysteresis loop with a slightly higher c_l during downstroke for the model with pure camber variation.

The c_d-Plots shown in Fig.13 reach their maximum at maximum AoA with a value of $c_{d,\,max} \approx 0,07$.

For the moment coefficient, depicted in Fig.14 we realized a nearly constant value over the whole periode with slight change in sign near the maximum AoA for the model according to Fig.6.

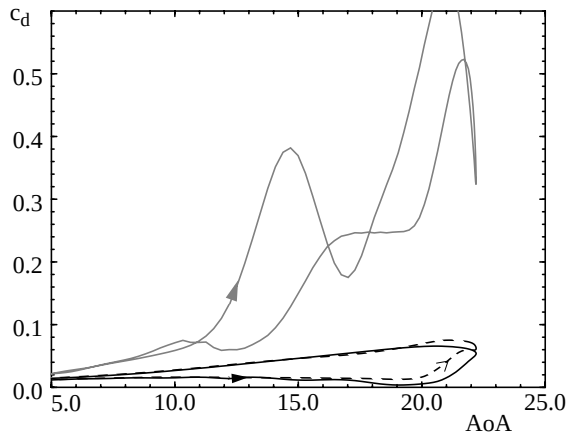

Fig.13 Drag coefficient vs. AoA for rigid airfoil, SSF and SCV airfoils

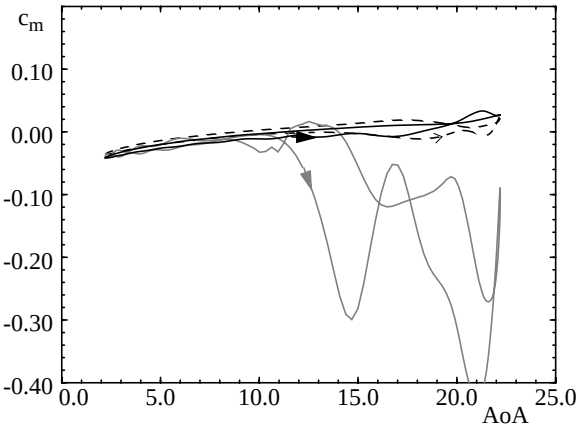

Fig.14 Moment coefficient vs. AoA for rigid airfoil, SSF and SCV airfoils

Because of the lack of any experimental results we decided to do some additional calculations with a different approach in modeling transition and turbulence.

As mentioned in [9]: “The incorporation of transitional flow effects using flow modeling was found to be a key element for an improved prediction of the dynamic stall hysteresis loops, even at relatively high Reynolds numbers.“

Therefore we correlate the transition onset point to the point on the airfoil where a minimum in pressure occurs. From this point on downstream we used the Chen-Thyson intermittency formulation to model the transition from laminar to turbulent boundary layer. For this kind of boundary layer treatment it was only possible to use the Baldwin-Lomax Turbulence Model so far.

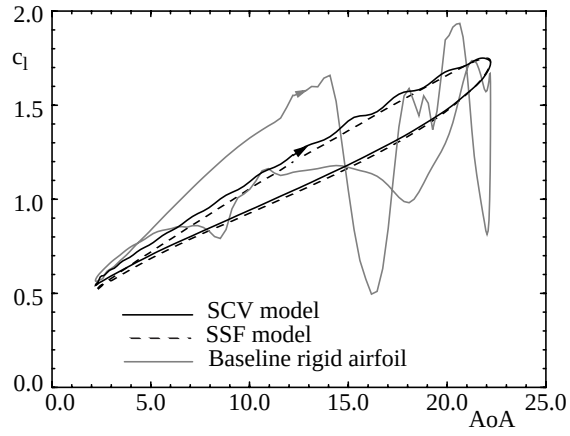

Fig.15 Lift coefficient vs. AoA for rigid airfoil, SSF and SCV airfoils, using Baldwin/Lomax turbulence model and Chen/Thyson transition model

As depicted in Fig.15 we get a rather similar result for the rigid airfoil with a slightly bigger decrease in c_l as the vortex looses contact with the airfoil and a higher lift overshoot near the highest AoA. For both deformed airfoils we achieve a very small hysteresis loop, indicating nearly suppressing the separation of dynamic stall vortex.

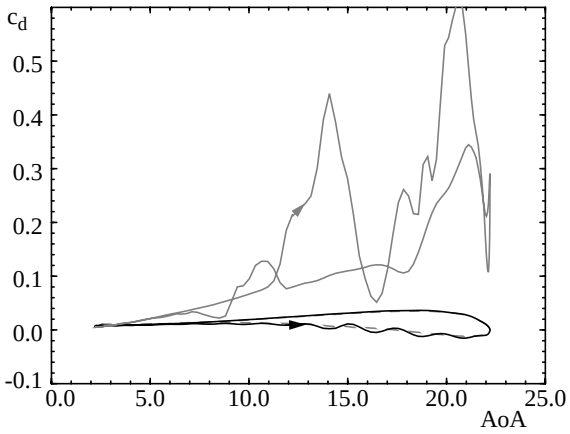

Fig.16 Drag coefficient vs. AoA for rigid airfoil and SSF and SCVairfoils, using Baldwin/Lomax turbulence model and Chen/Thyson transition model

We also realize the superimposed oscillation (Fig.15 to Fig.17) to be stronger as with the Spalart-Allmaras turbulence model during upstroke which comes from the effect of continuous compression and decompression areas at the upper leading edge as also shown in Fig.11.

In [11] a similar effect was found in experiments on the NACA0012 airfoil shown with Schlieren photographs.

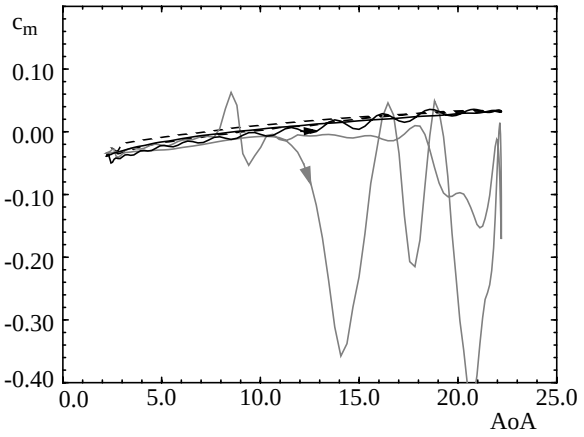

Fig.17 Moment coefficient vs. AoA for rigid airfoil, SSF and SCV airfoils, using Baldwin/ Lomax turbulence model and Chen/Thyson transition model

Unfortunately we could not get a converged solution for the baseline rigid airfoil with the transition onset at minimum pressure location, probably due to strong seperation over most of the airfoil upperside. We therefore used Michel's criterium to find the transition onset point.

Conclusions

Notwithstanding the need for a deepened theoretical modeling of unsteady aerodynamics including an extension of our inverse method of characteristics to become a 3D (= 2D unsteady) design tool, we have already a practical computational toolbox for improving given wing and blade sections. This is achieved by surface deformations resulting from realistic models of sealed slat (and flap) components and by local bump additions or subtractions as they result from steady shock-free design concepts, plus an application of the 'unsteady swept wing analogon' to calibrate parameters.

Two of our geometry models were tested for their effectiveness and ability in dynamic flow control.

Both models showed big potential in defining flow boundaries. As numerically demonstrated for the test case of dynamic stall control we think of our preprocessing tools as being able to deliver well developed models for time dependent flow boundary specifications.

It was found that modeling deformations using quintic functions for sealed slat and flap gives good results especially during the upstoke where the drooped nose dramatically reduces flow expansion and recompression shock strength.

From a practical point of view the SSF model may find a realization for adaptive helicopter rotor blades.

Modeling airfoil deformations by SCV airfoils still needs a more careful approach to find optimum parameters for the camber line variation. Some superimposed oscillations in the c_l-, c_d-, c_m-plots require further investigations. Low speed applications for the SCV model and suitable 3D geometry extensions can be found of course in modeling animal motions as for example flapping bird wings and fish bodies.

Also the approach in fixed wing aerodynamics controlling an airplane by changing the whole wing in a variable twist manner rather than the use of ailerons can be a field of interest for the SCV model with direct camber control.

Some uncertainties arise from numerical transition and turbulence modeling. As pointed out by many authors, taking care of the laminar boundary layer plays an important role in predicting dynamic stall. The lack of appropriate models still gives us only limited possibilities in exact prediction.

Various suitable computer visualization techniques, with video animation of the airfoil motion including flow separation, are found useful in trying to understand the physics of dynamic stall.

References

[1] Sobieczky, H., Seebass A. R.: Adaptive Airfoils and Wings for Shock-free Supercritical Flight. Invention Disclosure. University of Arizona Report EES TFD 78-02 (1978)

[2] Sobieczky, H.: Gasdynamic Knowledge Base for High Speed Flow Modelling. In: H. Sobieczky (Ed.), New Design Concepts for High Speed Air Transport. CISM Courses and Lectures Vol. 366. Wien, New York: Springer (1997), pp.105-120

[3] Sobieczky, H.: Parametric Airfoils and Wings. In: K. Fuji and G. S. Dulikravich (Eds.): Notes on Numerical Fluid Mechanics, Vol. 68, Wiesbaden: Vieweg (1998)

[4] Geissler, W., Sobieczky, H.: Unsteady Flow Control on Rotor Airfoils. AIAA 95-1890, (1995)

[5] Sobieczky, H.: Mathematische Modellbildung für komplexe Strömungsphänomene, Lecture Notes Technical University Vienna (1999)

[6] Sobieczky, H.: Analytical Tools for Systematic Transonic Design, IJNME Vol.22, (1986)

[7] Fung, K.-Y., Carr, L.: An Analytical Study of Compressibility Effects on Dynamic Stall. Frank Seiler Research Laboratory, FJSRL-TR 88-0004, (1988)

[8] Ekaterinaris, J. A., Platzer, M. F.: Numerical Investigation of Stall Flutter, Journal of Turbomachinery, Vol.118, (1996)

[9] Ekaterinaris, J. A., Platzer, M. F.: Computational Prediction of Airfoil Dynamic Stall. Prog. Aerospace Science, Vol. 33, (1997)

[10] Geissler, W., Trenker M., Sobieczky, H.: Active Dynamic Flow Control Studies on Rotor Blades. Paper at RTO AVT Panel Symposium “Active Control Technology for Enhanced Performance Operation Capabilities of Military Aircraft, Land Vehicles and Sea Vehicles”, Braunschweig, 8.-11. May 2000

[11] Carr, L. W., Chandrasekhara, M. S.: Compressibility Effects on Dynamic Stall, Prog. Aerospace Science, Vol. 32, (1996)